Dynamics of above-barrier state excitons in multi-stacked quantum dots

Kojima, Osamu
Tobita, Naoki
Kita, Takashi
Akahane, Kouichi

Dynamics of above-barrier state excitons in multi-stacked quantum dots

Osamu Kojima,[1,a)] Naoki Tobita,[1] Takashi Kita,[1] and Kouichi Akahane[2]
[1]*Department of Electrical and Electronic Engineering, Graduate School of Engineering, Kobe University, 1-1 Rokkodai, Nada, Kobe 657-8501, Japan*
[2]*National Institute of Information and Communications Technology, 4-2-1 Nukui-kitamachi, Koganei, Tokyo 184-8795, Japan*

(Received 8 February 2011; accepted 30 September 2011; published online 10 November 2011)

We report the relaxation dynamics from above-barrier exciton states to the lowest one in multi-stacked quantum dots (QDs). The photoluminescence decay time increases because of the excitation of higher exciton states, which is attributed to the wider miniband width of above-barrier excitons and the localization of the envelope functions in the barrier layers. The existence of the above barrier minibands makes carrier transport along the growth direction possible and eliminates a difficulty with close QD stacking. These results demonstrate an effective approach to achieve high efficiency QD devices. © *2011 American Institute of Physics*. [doi:10.1063/1.3660210]

I. INTRODUCTION

Quantum dots (QDs) on semiconductor substrates are the most promising platforms to achieve QD lasers,[1] ultrafast optical switches,[2,3] and solar cells.[4,5] We have already shown the advantages of stacked QDs grown by using a strain compensation technique[6–8] for controlling the optical characteristics and the fabrication of high-density QD ensembles.[9–11]

In our recent report, the existence of high exciton states above the barrier height in stacked QDs has been demonstrated by examining the excitation-energy dependence of the photoluminescence (PL) intensity; the excitation of these higher states significantly enhances the PL intensity.[12] Thus, the clarification of the carrier dynamics from these above-barrier states to the lowest exciton state is considered valuable for realizing high-efficiency QD devices. In this study, we investigated the PL dynamics from the above-barrier states to the lowest exciton ones in multi-stacked QDs that were fabricated using a strain compensation technique. The excitation of the above-barrier states increases the PL decay time from the lowest exciton in the thicker spacer layer sample. A rate-equation analysis shows that this phenomenon can be explained in terms of the relaxation time from the higher states to the lowest ones. We discuss the dynamics in terms of the above-barrier minibands.

II. EXPERIMENT

We used two samples in this study. For each sample, InAs self-assembled QDs with 30 layers were grown on an InP(311)B substrate by molecular beam epitaxy by using the strain compensation technique.[10] We deposited 4-ML InAs QDs on a 150-nm-thick $In_{0.52}Al_{0.48}As$ buffer layer. The samples have $In_{0.5}Ga_{0.1}Al_{0.4}As$ spacer layers with thicknesses of 20 and 40 nm. The QD density in each sample is $2.5 \times 10^{12}/cm^2$. Hereafter, we denote them as $d = 20$ nm and $d = 40$ nm samples, respectively. According to our previous report,[10] in the $d = 20$ nm sample, the QDs are interconnected along the growth direction, which increases the exciton lifetime by decreasing the oscillator strength. The spacer layer compensates for the stress caused by the lattice mismatch between the QD and the buffer layers. The PL decay profiles were measured using a time-correlated single-photon counting method with a time resolution of 0.8 ns estimated by the width of the measured laser pulse waveform. The excitation source was a mode-locked Ti:sapphire pulse laser delivering 110-fs pulses with a repetition rate of 4 MHz. We used a pulse picker to reduce the laser repetition rate from 80 to 4 MHz. The excitation photon energy was 1.550 eV, and the excitation density was kept at 0.22 $\mu J/cm^2$. On the other hand, to excite the higher excitonic state in the $d = 40$ nm sample, we used the second-harmonic light of an optical parametric oscillator excited by a mode-locked Ti:sapphire pulse laser with a repetition rate of 80 MHz and pulse width of 120 fs. To eliminate the high-density excitation effect of 80 MHz excitation, the excitation density was kept at 2.2 nJ/cm^2, which corresponds to the excitation of one QD by one photon. PL was dispersed using a 27 cm single monochromator with a resolution of 1.0 nm and was detected using a time-to-amplitude converter system with a liquid-nitrogen-cooled InP/InGaAsP photomultiplier. The PL spectrum of the spacer layer in each sample was measured by using the semiconductor laser with the energy of 1.907 eV. The excitation density was 0.05 W/cm^2. All measurements were performed at low temperature.

III. RESULTS AND DISCUSSION

The PL intensity in the $d = 40$ nm and $d = 20$ nm samples is plotted as a function of excitation energy in Fig. 1.[12] The PL intensities were normalized by the maximum intensity in each sample. For reference, the PL spectra are shown. In this measurement, the number of excitation photon was kept constant. The bandgap energy of the InP substrate is 1.424 eV at 1.6 K.[13] The PL spectra of the $In_{0.5}Ga_{0.1}Al_{0.4}As$ spacer layer in both samples show a peak at 1.435 eV as depicted by the dotted curves. Therefore, we considered that the peaks of the excitation-energy dependence of the PL

a)Author to whom correspondence should be addressed. Electronic mail: kojima@phoenix.kobe-u.ac.jp.

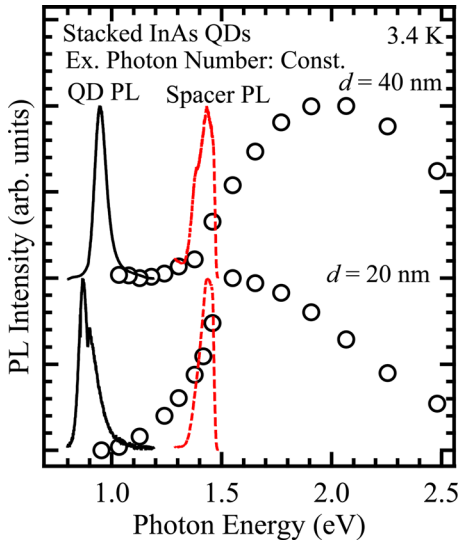

FIG. 1. (Color online) Excitation-energy dependence of the PL intensity in the $d = 40$ and $d = 20$ nm samples (Ref. 12). The dotted curves indicate the PL spectra of the spacer layer.

intensity originate not from the spacer layers but from higher-state excitons.

To clarify the characteristics of these higher exciton states, we measured the PL decay profiles. Figure 2(a) shows the excitation-energy dependence of the PL decay profile in the $d = 40$ nm sample. All the profiles were recorded at the

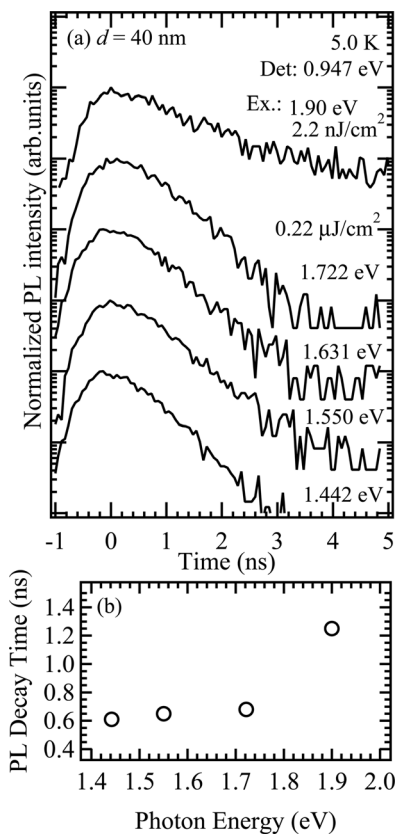

FIG. 2. (a) Excitation-energy dependence of the PL decay profiles in the $d = 40$ nm sample. Detection energy is the PL peak energy of the sample. Excitation energy at 1.90 eV corresponds to the excitation of higher states. (b) PL decay time plotted as a function of excitation energy.

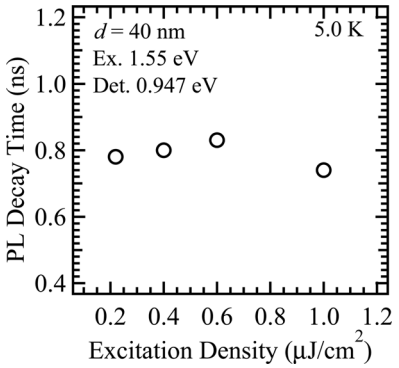

FIG. 3. Excitation-density dependence of the PL decay time in the d = 40 nm sample.

PL peak energy. The PL decay time excited at 1.90 eV increases rapidly. In Fig. 2(b), the PL decay time evaluated by fitting with a single exponential function form was plotted as a function of excitation energy. Although the PL decay time is almost constant at approximately 0.7 ns at excitation energies below 1.8 eV, the PL decay time at excitation energy of at 1.90 eV increases up to 1.25 ns.

To explain the increase in the PL decay time, we considered the high density effect of excitons due to the use of a high-repetition-rate pulse laser. Figure 3 shows the excitation density dependence of the PL decay time in the $d = 40$ nm sample. The excitation energy was 1.55 eV, and the detection energy was the PL peak energy. The PL decay time hardly depends on the excitation density in our measurement region. Moreover, as mentioned above, a QD was excited by one photon in the measurement of excitation at 1.90 eV. Therefore, the excitation density, i.e., the carrier accumulation, does not affect the PL decay time.

Next, we considered the effect of carrier transfer from smaller QD to larger one. In the case of the thicker spacer sample, the QD separation along the growth direction is larger than that in the in-plane direction. To clarify the effect of carrier transfer in the in-plane direction, we examined the detection-energy dependence of the PL decay profiles at excitation energies of 1.90 and 1.55 eV. Figure 4 plots the PL decay time as a function of the detection energy. Clearly, the

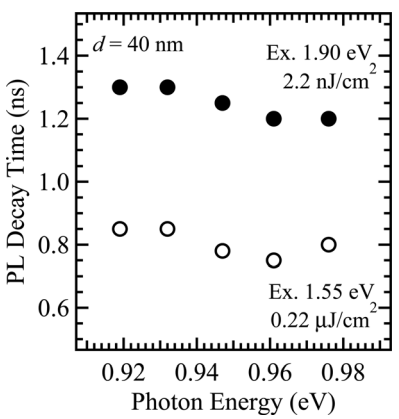

FIG. 4. Detection-energy dependence of the PL decay time. Closed and open circles indicate the results for excitation at 1.90 and 1.55 eV, respectively.

PL decay times at both excitation energies hardly depend on the detection energy. The result obtained at the excitation energy of 1.55 eV is consistent with our previous result, in which the PL decay time at a low temperature of 3.4 K is almost constant.[10] Surprisingly, the PL decay time at the excitation energy of 1.90 eV is also independent of the detection energy. Therefore, the change in the PL decay time in Fig. 2 does not originate in the carrier transfer between QDs.

Since the exciton accumulation effect and carrier transfer were denied, the lengthening of the PL decay time does not originate from the interaction between the lowest excitons in the QDs, and that can be attributed to relaxation from a higher exciton state. Thus, we performed an analysis based on the rate equations. The rate equations are defined as follows:

$$\frac{dn_2(t)}{dt} = -\gamma_2 n_2(t), \tag{1}$$

$$\frac{dn_1(t)}{dt} = -\gamma_1 n_1(t) + \gamma_2 n_2(t), \tag{2}$$

where $n_1(t)$ and $n_2(t)$ are the populations in the exciton and higher exciton states, respectively, and γ_1 and γ_2 are the respective relaxation rates for those states. Moreover, C_1 and C_2 are the populations generated by the pulse. The analytical solution of these equations for $n_1(t)$ is

$$n_1(t) = \frac{C_2\gamma_2}{\gamma_1 - \gamma_2}\exp(-\gamma_2 t) + C_1\exp(-\gamma_1 t). \tag{3}$$

In a numerical simulation using this equation, we used $\gamma_1 = 1/0.8$/ns, and C_1, C_2, and γ_2 were used as parameters.

Figure 5(a) shows the results for various C_2 values under $\gamma_2 > \gamma_1$. In all the results in Fig. 5, the PL rise due to intraband relaxation was neglected, which does not affect the decay time from the n_1 state. All profiles were normalized by the maximum intensity. Open circles demonstrate the numerically reproduced experimental result with γ_1. For all values of C_2, the profiles decay by γ_1. Therefore, γ_2 should be smaller than γ_1. Figure 5(b) shows the results for various C_2 values under $\gamma_2 < \gamma_1$. When $C_1 > C_2$, the profile decays by γ_1. On the other hand, when $C_2 > C_1$, the profiles decay by γ_2, which agrees with the experimental results. $C_2 > C_1$ corresponds to resonant excitation at the higher exciton state. Figure 5(c) demonstrates the results for various γ_2 at $C_2 = C_1$. In this case, the profiles show a double exponential form. From these results, we concluded that $\gamma_2 = 1/1.3$/ns; the relaxation time from the higher exciton state to the exciton state is approximately 1.3 ns.

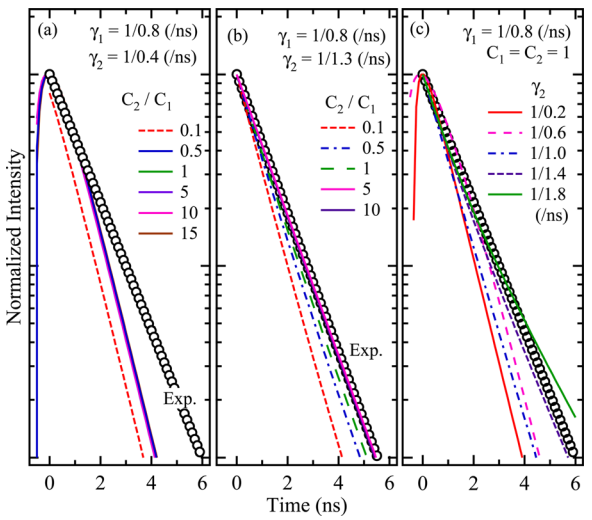

FIG. 5. (Color online) Numerical simulation of the PL decay profiles described by Eq. (3). (a) For various C_2 under $\gamma_1 < \gamma_2$, (b) for various C_2 under $\gamma_1 > \gamma_2$, and (c) for various γ_2 under $C_1 = C_2$. Open circles represent the numerically reproduced experimental results.

Here, we discuss the origin of the higher exciton states from these results. The possibility of a biexciton is immediately eliminated by the relaxation time. In multiple quantum wells, above-barrier excitons have been reported.[14–20] These excitons have two significant features: (i) broadening of the miniband width and (ii) localization of the wave functions in barrier layers. It is well-known that the miniband width depends on the subband order.[21] The wider miniband means the stronger coupling between the envelope functions in QDs; the coupling distance of the envelope functions between related QDs increases. Therefore, the further expansion of the envelope functions of electrons and holes along the growth direction is possible. In QD systems, hole localization is stronger than electron localization because of the greater mass.[22] Therefore, electron relaxation to a lower state under the above-barrier excitation condition becomes longer than that under the below-barrier condition. Moreover, the localization of the envelope functions of the above-barrier-minibands in the barrier layers in strained-quantum wells is one factor that increases the relaxation time to the lower states.[16,17,20] These two factors increase the PL decay time excited at the higher state.

Unfortunately, to our knowledge, there is no reference to explain the theoretical reason of the increase in the PL decay time due to the increase in the intraband relaxation time. Thus, we speculate the increase in the intraband relaxation time on the basis of the potential profiles. Assuming the strain distribution calculated by Grundmann in and around a pyramidal InAs QD,[23] there exist lateral potentials for electrons and holes in the vicinity of a dot. The potential increases close to the dot and gives rise to a barrier for the capture of carriers in the spacer layers. The spatially modulated potential profiles lead to the indirect intraband transitions from the spacer layers to QDs. This situation is similar to the interband transition in the nipi structures. In the nipi structures, Dohler's model describes the indirect transition time as $\tau_{ind} = \tau_d \exp(\Delta E/kT)$, where τ_d is the direct transition time in bulk crystals, ΔE is the energy difference between the direct transition and indirect transition, k is the Boltzmann factor, and T is the temperature.[24] As the band offset ratio between the QD exciton states and the above exciton states, we assumed the offset ratio as 0.7. The energy difference between the QD exciton and the above barrier exciton is 1.1 eV so that the indirect intraband relaxation time is enhanced by a factor of 13 (3) for electron (hole) at 3.4 K. Although this assumption is insufficient to describe the correct physical model, the tendency of the increase in the intraband relaxation time can explain qualitatively.

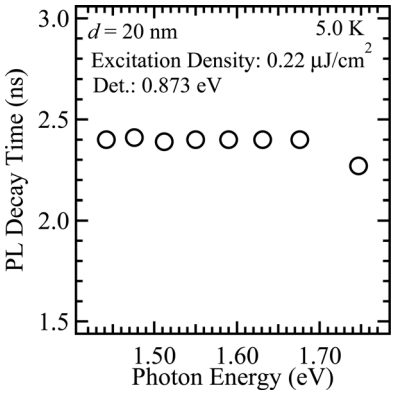

FIG. 6. PL decay time evaluated by fitting with a single exponential function form plotted as a function of excitation energy in the d = 20 nm sample. The detection energy is the PL peak energy.

Finally, we discuss the relation between the lifetime of the lowest exciton and the dynamics of the above-barrier excitons. As we have reported, the decrease in d induces the elongation of the electron envelope functions along the growth direction, which leads to the lowering of the oscillator strength.[10] Namely, the exciton lifetime in the $d = 20$ nm sample is longer than that in the $d = 40$ nm sample because of the interconnection effects. Figure 6 shows the excitation-energy dependence of the PL decay time in the $d = 20$ nm sample. Although the excitation energies are less than 1.90 eV which is the excitation energy in the $d = 40$ nm sample the excitation energies over 1.631 eV are enough to excite the higher states in the $d = 20$ nm as shown in Fig. 1. The PL decay time is almost constant. In the $d = 20$ nm sample, the exciton lifetime is increased by the elongation of the electron envelope function, which is comparable to the relaxation time from the higher states to the exciton states. Thus, the PL decay time is independent of the excitation energy.

IV. CONCLUSION

We have investigated the effects of the excitation of higher exciton states on the PL decay time of excitons in stacked QDs fabricated using a strain compensation technique. We found that the PL decay time excited at the higher exciton state significantly increases in the $d = 40$ nm sample. To clarify the origin of this phenomenon, we examined the excitation-power dependence and the detection-energy dependence of the PL decay time. These measurements clearly eliminated the effect of carrier accumulation and carrier transfer between QDs as the origin of the lengthening of the PL decay time. Moreover, the analysis based on the rate equations shows that the relaxation time from the higher exciton states to the lowest exciton state is much longer than the exciton lifetime, which explains the increase in the PL decay time. The two features of the above-barrier minibands are important factors in explaining our results: (i) broadening of the miniband width and (ii) localization of the wave functions in barrier layers. In contrast, in the $d = 20$ nm sample, the PL decay time excited at higher exciton states hardly shows lengthening because of long exciton lifetime due to the interconnection effects. These may facilitate the development of functional devices by using QDs. In particular, the existence of the above-barrier minibands makes it possible to transport carriers along the growth direction and eliminates a difficulty with close QD stacking.

ACKNOWLEDGMENTS

This work was partially supported by Grants-in-Aid for Scientific Research from the Ministry of Education, Culture, Sports, Science, and Technology (MEXT) of Japan, for Scientific Research on Innovative Areas "Optical Science of Dynamically Correlated Electrons" from MEXT of Japan, the Incorporated Administrative Agency New Energy and Industrial Technology Development Organization, and Ministry of Economy, Trade, and Industry, Japan.

[1] D. L. Huffaker, G. Park, Z. Zou, O. B. Shchekin, and D. G. Deppe, Appl. Phys. Lett. **73**, 2564 (1998).
[2] R. Prasanth, J. E. M. Haverkort, A. Deepthy, E. W. Bogaart, J. J. G. M. van der Tol, E. A. Patent, G. Zhao, Q. Gong, P. J. van Veldhoven, R. Nötzel, and J. H. Wolter Appl. Phys. Lett. **84**, 4059 (2004).
[3] E. W. Bogaart, R. Nötzel, Q. Gong, J. E. M. Haverkort, and J. H. Wolter, Appl. Phys. Lett. **86**, 173109 (2005).
[4] A. Martí, E. Antolín, C. R. Stanley, C. D. Farmer, N. López, P. Díaz, E. Cánovas, P. G. Linares, and A. Luque, Phys. Rev. Lett. **97**, 247701 (2006).
[5] R. Oshima, A. Takata, and Y. Okada, Appl. Phys. Lett. **93**, 083111 (2008).
[6] K. Akahane, N. Ohtani, Y. Okada, and M. Kawabe, J. Cryst. Growth **245**, 31 (2002).
[7] K. Akahane, N. Yamamoto, and M. Tsuchiya, Appl. Phys. Lett. **93**, 041121 (2008).
[8] K. Akahane, N. Yamamoto, and T. Kawanishi, Phys. Status Solidi A **208**, 425 (2011).
[9] H. Nakatani, T. Kita, O. Kojima, O. Wada, K. Akahane, and M. Tsuchiya, J. Lumin. **128**, 975 (2008).
[10] O. Kojima, H. Nakatani, T. Kita, O. Wada, K. Akahane, and M. Tsuchiya, J. Appl. Phys. **103**, 113504 (2008).
[11] O. Kojima, H. Nakatani, T. Kita, O. Wada, and K. Akahane, J. Appl. Phys. **107**, 073506 (2010).
[12] O. Kojima, M. Mamizuka, T. Kita, O. Wada, and K. Akahane, Phys. Status Solidi C **8**, 46 (2011).
[13] O. Madelung, in *Semiconductors: Data Handbook* (Springer, Berlin, 2004).
[14] C. Weisbuch and B. Vinter, in *Quantum Semiconductors Structures* (Academic, Boston, 1991).
[15] F. C. Zhang, N. Dai, H. Luo, N. Samarth, M. Dorobrowolska, J. K. Furdynna, and L. R. Ram-Mohan, Phys. Rev. Lett. **68**, 3220 (1992).
[16] F. Martelli, M. Capizzi, A. Frova, A. Polimeni, F. Sarto, M. R. Bruni, and M. G. Simeone, Phys. Rev. B **48**, 1643 (1993).
[17] M. Cappizi, A. Polimeni, A. Frova, F. Martelli, K. B. Ozanyan, T. Worren, M. R. Bruni, and M. G. Simeone, Solid-State Electron. **37**, 641 (1994).
[18] M. Nakayama, R. Sugie, H. Ohta, and S. Nakashima, Jpn. J. Appl. Phys. **34**, Suppl. 34-1, 80 (1995).
[19] M. Nakayama, M. Andou, I. Tanaka, H. Nishimura, H. Schneider, and K. Fujiwara, Phys. Rev. B **51**, 4236 (1995).
[20] T. Worren, K. B. Ozanyan, O. Hunderi, and F. Martelli, Phys. Rev. B **58**, 3977 (1998).
[21] T. Hasegawa and M. Nakayama, Jpn. J. Appl. Phys. **44**, 8340 (2005).
[22] W. Jaskólslo, M. Zieliński, G. W. Bryant, and J. Aizpurua, Phys. Rev. B **74**, 195339 (2006).
[23] M. Grundmann, O. Stier, and D. Bimberg, Phys. Rev. B **52**, 11969 (1995).
[24] Z. J. Yang, E. M. Garmire, and D. Doctor, J. Appl. Phys. **82**, 3874 (1997).